

# Developing a Multi-channel Beamformer by Enhancing Spatially Constrained ICA for Recovery of Correlated EEG Sources

Nasser Samadzadehghdam<sup>1,2</sup>, Bahador MakkiAbadi<sup>1,3,\*</sup>, Ehsan Eqlimi<sup>4,5</sup>, Fahimeh Mohagheghian<sup>6</sup>, Hassan Khajehpoor<sup>1,3</sup>, Mohammad Hossein Harirchian<sup>7</sup>

## ABSTRACT

**Background:** Brain source imaging based on electroencephalogram (EEG) data aims to recover the neuron populations' activity producing the scalp potentials. This procedure is known as the EEG inverse problem. Recently, beamformers have gained a lot of consideration in the EEG inverse problem.

**Objective:** Beamformers lack acceptable performance in the case of correlated brain sources. These sources happen when some regions of the brain have simultaneous or correlated activities such as auditory stimulation or moving left and right extremities of the body at the same time. In this paper, we have developed a multi-channel beamformer robust to correlated sources.

**Material and Methods:** In this simulation study, we have looked at the problem of brain source imaging and beamforming from a blind source separation point of view. We focused on the spatially constraint independent component analysis (scICA) algorithm, which generally benefits from the pre-known partial information of mixing matrix, and modified the steps of the algorithm in a way that makes it more robust to correlated sources. We called the modified scICA algorithm Multichannel ICA based EEG Beamformer (MIEB).

**Results:** We evaluated the proposed algorithm on simulated EEG data and compared its performance quantitatively with three algorithms: scICA, linearly-constrained minimum-variance (LCMV) and Dual-Core beamformers; it is considered that the latter is specially designed to reconstruct correlated sources.

**Conclusion:** The MIEB algorithm has much better performance in terms of normalized mean squared error in recovering the correlated/uncorrelated sources both in noise free and noisy synthetic EEG signals. Therefore, it could be used as a robust beamformer in recovering correlated brain sources.

**Citation:** Samadzadehghdam N, MakkiAbadi B, Eqlimi E, Mohagheghian F, Khajehpoor H, Harirchian MH. Developing a Multi-channel Beamformer by Enhancing Spatially Constrained ICA for Recovery of Correlated EEG Sources. *J Biomed Phys Eng.* 2021;11(2):205-214. doi: 10.31661/jbpe.v010.801.

## Keywords

ICA Based Beamformer; Correlated Sources Recovery; Signal Processing, Computer-Assisted; Electroencephalography; Brain Waves

## Introduction

The aim of brain source imaging is to find areas of the brain and their corresponding activities responsible for the observed EEG. This process is composed of two steps: the forward problem and inverse problem. Forward problem solution aims to define a volume conductor model for the head by which the scalp EEG potentials are generat-

<sup>1</sup>PhD, Department of Medical Physics and Biomedical Engineering, School of Medicine, Tehran University of Medical Sciences (TUMS), Tehran, Iran

<sup>2</sup>PhD, Department of Medical Bioengineering, Faculty of Advanced Medical Sciences, Tabriz University of Medical Sciences, Tabriz, Iran

<sup>3</sup>PhD, Research Center for Biomedical Technology and Robotics (RCBTR), Institute of Advanced Medical Technologies (IAMT), Tehran University of Medical Sciences (TUMS), Tehran, Iran

<sup>4</sup>PhD Candidate, Department of Medical Physics and Biomedical Engineering, School of Medicine, Tehran University of Medical Sciences (TUMS), Tehran, Iran

<sup>5</sup>PhD Candidate, Research Center for Biomedical Technology and Robotics (RCBTR), Institute of Advanced Medical Technologies (IAMT), Tehran University of Medical Sciences (TUMS), Tehran, Iran

<sup>6</sup>PhD, Department of Medical Physics and Biomedical Engineering, School of Medicine, Shahid Beheshti University of Medical Sciences, Tehran, Iran

<sup>7</sup>MD, Iranian Centre of Neurological Research, Neuroscience Institute, Tehran University of Medical Sciences, Tehran, Iran

\*Corresponding author: Bahador MakkiAbadi  
Research Center for Biomedical Technology and Robotics (RCBTR), Institute of Advanced Medical Technologies (IAMT), Tehran University of Medical Sciences (TUMS), Tehran, Iran  
E-mail: b-makkiabadi@sina.tums.ac.ir

Received: 25 June 2017  
Accepted: 14 October 2017

ed for the given neural sources namely current dipoles. The first and less computational model was a three shell concentric spherical head model in which the inner sphere represents the brain, the intermediate layer represents the skull and the outer layer represents the scalp. More realistic head models are obtained using MRI/CT 3D images to extract different conducting compartments associated with certain tissues [1]. Boundary element method (BEM), the finite element method (FEM) and the finite difference method (FDM) are three numerical methods which have been used to solve Poisson's equation in a realistically shaped head model [2] which results to the Lead Field Matrix (LFM). This matrix shows the sensitivity of the surface electrodes to particular unit-magnitude current sources located inside the brain.

The second step i.e. inverse solution deals with identifying the source signals from noisy EEG measurements. Although solving the forward problem has become straightforward, finding a solution to the inverse problem, due to its underdetermined mixing scenario, is still a challenging task. Different classifications are provided for inverse algorithms literature. Grech, et al. [3] discussed the methods in parametric vs. non-parametric categories. The main difference between the two is to whether a fixed number of dipoles is assumed a priori or not [3]. The source imaging methods, which are based on minimum-norm minimization, and their generalizations such as LORETA and sLORETA [4] fall into non-parametric category, while beamforming techniques and MUSIC [5] algorithm are classified as parametric. Sekihara and Nagarajan [6] categorized the algorithms in adaptive and non-adaptive spatial filters (beamformers) depending on whether the beamformer parameters depend only on the geometry of the measurements or on the temporal EEG information too. Jonmohamadi et al. [7] compared 8 beamformers with respect to several parameters including variations in depth, orientation, magnitude, and

the frequency of the simulated sources to determine their effectiveness at the time course of reconstructed sources and stability of their performances with respect to the input parameter variations. They concluded that, although minimum-variance beamformers were more sensitive to changes into magnitude, depth, and frequency of the simulated source, they had higher gains and superior spatial resolution to those of the minimum-norm beamformers. Conventional beamformers such as LCMV act well in reconstructing uncorrelated sources [8], but they are poor at reconstructing correlated sources [9].

To handle the problem of source correlation, Georgieva et al. [10] proposed a method combining a particle filter (statistical approach) for estimation of the spatial location and a multicore beamformer (deterministic approach) for estimation of temporally correlated dipole waveforms in a recursive framework. Subsequently, Brookes et al. [11] proposed dual source beamformer, for imaging two temporally correlated sources, based on the beamformer technique. Another method for recovering dynamics of temporally correlated neural sources was combining LCMV beamformer with the surface Laplacian [8]. Surface Laplacian, is the second spatial derivative of the scalp EEG and in fact, reduces the effects of low skull conductivity. A "Dual-Core Beamformer" (DCBF) technique [9] in conjunction with a modified Powell algorithm, calculates optimal amplitude-weighting and dipole orientation for reconstruction and, therefore, has much less computational cost compared to the dual-beamformer technique.

In this paper, we aim to develop a new beamformer based on BSS techniques namely spatially constraint ICA, for reconstructing correlated brain sources. In section 2 we will discuss briefly about the theory of LCMV, sICA and will address our proposed modifications to increase the robustness to correlated sources. The simulation results are provided in section 3. Finally, we will go through the

discussion in section 4.

### Material and Methods

In this simulation study, a linear model is assumed for EEG signals, then, the basis of the developed beamformer is explained and evaluated by the synthetic EEG.

It seems reasonable to assume that the measured scalp EEGs at time  $t$  is a  $M \times I$  vector,  $\mathbf{x}(t)$ , where  $M$  is the total number of surface electrodes. If  $\mathbf{s}$  is defined as the source dipole at location  $\mathbf{r}$ , then the relation between measured data and  $\mathbf{s}(\mathbf{r}, t)$  is given by;

$$\mathbf{x}(t) = \mathbf{L}(\mathbf{r})\mathbf{s}(\mathbf{r}, t) \tag{1}$$

Where,  $\mathbf{s}(\mathbf{r}, t)$  is a  $3 \times I$  column vector at time  $t$  and its elements represent the  $x$ ,  $y$  and  $z$  components of the dipole momentum.  $\mathbf{r}=(x,y,z)$ ' is the  $3 \times I$  location vector and  $\mathbf{L}$  is the  $M \times 3$  the lead field matrix obtained from the forward problem solution and indicates the sensitivity of the sensor array to a particular unit-magnitude source located at  $\mathbf{r}$  [6].

Now, it can be supposed that the number of active dipole sources is  $K$ . Then, the superposition of  $K$  potential fields generated by these  $K$  sources could be applied due to the linearity assumption of head model medium [12] as follows;

$$\mathbf{x}(t) = \sum_{i=1}^K \mathbf{L}(\mathbf{r}_i)\mathbf{s}(\mathbf{r}_i, t) + \mathbf{n}(t) \tag{2}$$

In which  $\mathbf{n}(t)$  is a  $M \times I$  vector at time  $t$  denoting sensor level additive Gaussian white noise.

The ultimate goal in EEG inverse problem is to estimate  $\mathbf{s}(\mathbf{r}, t)$  using measurement  $\mathbf{x}(t)$  and the lead field matrix  $\mathbf{L}(\mathbf{r})$ .

#### LCMV beamformer

A spatial filter, which is often called a beamformer in signal processing contexts [6], can estimate the neural power originating within its spatial pass-band while suppressing the activity of other locations. Moving the filter pointing location throughout brain voxels a

spatial pattern of neural activity or power as a function of brain location is acquired. The pattern of neural power can be used for solving the source localization problem, such that the regions with the highest neural power would be interpreted as the source location.

The strategy of spatial filter is to design a  $M \times 3$  weight matrix or filter  $\mathbf{W}(\mathbf{r})$  which can reconstruct the brain source signal using the sensor array  $\mathbf{x}(t)$ , such that,

$$\hat{\mathbf{s}}(\mathbf{r}, t) = \mathbf{W}^T(\mathbf{r})\mathbf{x}(t) \tag{3}$$

where,  $\hat{\mathbf{s}}(\mathbf{r}, t)$  is the reconstructed source located at  $\mathbf{r}$ , in the center of filter pass-band and is an estimation of the original source.

The activity level or power of a specific source can be determined by its variance. The LCMV weights are determined imposing the minimum variance constraint on its output. The most common way to obtain the variance of filter output is to sum the variance of its components as below;

$$\text{Var}(\hat{\mathbf{s}}(\mathbf{r}, t)) = \text{tr} \mathbf{C}(\hat{\mathbf{s}}(\mathbf{r}, t)) \tag{4}$$

Where  $\mathbf{C}(\hat{\mathbf{s}}(\mathbf{r}, t))$  denotes the covariance matrix of the estimated source and  $\text{tr}(\cdot)$  is the trace operator of matrix.

Then the fundamental goal is to find weight matrix  $\mathbf{W}$  such that [13].

$$\min_{\mathbf{w}(\mathbf{r})} \text{tr} \mathbf{C}(\hat{\mathbf{s}}(\mathbf{r}, t)) \quad \text{subject to } \mathbf{W}^T(\mathbf{r})\mathbf{L}(\mathbf{r}) = \mathbf{I} \tag{5}$$

The above optimization problem can ensure that the signals generated pass at location  $\mathbf{r}$  through the filter while suppressing all other signals.

Substituting equation (4) into equation (5):

$$\min_{\mathbf{w}(\mathbf{r})} \text{tr}(\mathbf{W}^T(\mathbf{r})\mathbf{C}(\mathbf{x}(t))\mathbf{W}(\mathbf{r})) \quad \text{subject to } \mathbf{W}^T(\mathbf{r})\mathbf{L}(\mathbf{r}) = \mathbf{I} \tag{6}$$

Where  $\mathbf{C}(\mathbf{x}(t))$  is the covariance matrix of measured data vector  $\mathbf{x}(t)$ .

By solving the above constraint minimization problem using Lagrangian method, the weight vector satisfying (6) is given by:

$$\mathbf{W}(\mathbf{r}) = \mathbf{C}^{-1}(\mathbf{x}(t))\mathbf{L}(\mathbf{r})[\mathbf{L}^T(\mathbf{r})\mathbf{C}^{-1}(\mathbf{x}(t))\mathbf{L}(\mathbf{r})]^{-1} \quad (7)$$

It has been shown that conventional beamformer techniques have a weak performance in reconstructing correlated sources [8, 9, 14].

As mentioned in the introduction, some improvements have been made in order to enhance the beamformer performance in reconstructing correlated sources. One of the recent algorithms is Dual-Core beamformer (DCBF) which is a spatial filter with two cores rather than one. Since one of the major contributions of the enhanced algorithm is in reconstructing correlated sources we have compared our results with this algorithm, too. For more details about DCBF, it can be referred to [9].

### scICA

Independent component analysis (ICA) is a blind source separation (BSS) algorithm for separating a set of independent mixed signals into additive subcomponents, without having any information about mixing process. However, it is possible to incorporate any possible prior information such as source temporal information [15] or spatial constraints related to the mixing process [16, 17] leading to semi-blind or constrained separating algorithms. In the case of ICA, it is assumed that at most one of the components may have Gaussian distribution and all of them are statistically independent of each other.

Standard formulations of the ICA can be shown as follows.

$$\mathbf{X} = \mathbf{A}\mathbf{S} + \mathbf{N} \quad (8)$$

Rows of matrix  $\mathbf{X}$  is the time series of the  $M$  measured signals which are a linear combination of  $K$  source signals which cannot be observed directly and lay in the rows of matrix  $\mathbf{S}$ . Matrix  $\mathbf{N}$  represents additive noise.

Here, we are going to address EEG inverse problem as a BSS problem. This is possible by replacing the mixing matrix with the lead field matrix in equation (8). In fact, if we are interested in some dominant neural sources for

which we have a prior knowledge about their location, we can replace their corresponding columns from the lead field matrix into the mixing matrix.

Recovering source signals requires a demixing matrix such that:

$$\hat{\mathbf{S}} = \hat{\mathbf{P}}\mathbf{X} \quad (9)$$

In which  $\hat{\mathbf{S}}$  denotes the estimated source waveform. While mixing matrix,  $\mathbf{A}$ , has been estimated,  $\hat{\mathbf{p}}$  could be obtained from pseudo inverse, minimum mean square estimate (MMSE) [18] and maximum a posteriori (MAP) or ML approaches [19] depending on  $M$ ,  $K$  and conditions of noise. Estimating the mixing matrix generally involves an optimization problem with the aim of minimizing the mutual dependence of the source estimates with reference to higher order statistics or information theoretic measures [16].

Popular ICA algorithms include JADE [20], SOBI [21] FastICA [22] as well as Bayesian based approaches [23].

In the spatially constrained ICA algorithm (scICA), as a semi-blind source separation algorithm, proposed in [17], it is supposed that the mixing matrix information is known for one or several sources. Here we provide this prior information from the lead field matrix obtained from the solution of EEG forward problem. The algorithm is composed of the following steps.

The first step is the dimensionality reduction of the observed data. Computing the orthogonal basis of the  $J$  known mixing vectors,  $\tilde{\mathbf{U}}_{1:J}$ , the observed data is projected on the orthogonal complement of this basis as follows:

$$\mathbf{X}_2 = (\mathbf{I} - \tilde{\mathbf{U}}_{1:J}\tilde{\mathbf{U}}_{1:J}^H)\mathbf{X} \quad (10)$$

Then the data is projected on matrix  $\tilde{\mathbf{U}}$  whose  $J+1:K$  columns are  $K-J$  dominant left singular vectors of  $\mathbf{X}_2$ :

$$\mathbf{X}_s = \tilde{\mathbf{U}}^H\mathbf{X} \quad (11)$$

The next step is whitening the observed data

and the known mixing vectors:

$$\mathbf{X}_w = \mathbf{P}^\dagger \mathbf{Q}^H \cdot \mathbf{X}_s \quad (12)$$

$$\mathbf{v}_l = \mathbf{P}^\dagger \mathbf{Q}^H \cdot \tilde{\mathbf{U}}^H, \quad l = 1 \dots J \quad (13)$$

In which  $\mathbf{Q}$  and  $\mathbf{P}$  are obtained from eigenvalue decomposition (EVD) of the covariance matrix of  $\mathbf{X}_s$ .

$\mathbf{v}_l$  columns are normalized to unit length and should be column-wise orthonormal while staying as close as possible to the known vectors [17]. This is accomplished through an iterative step which minimizes  $\|\mathbf{v}_{1:J} \cdot \mathbf{D} - \mathbf{Z}\|^2$ .

$\mathbf{D}$  is a diagonal matrix and  $\mathbf{v}_l$  is replaced with  $\mathbf{Z}$ . Computing its orthogonal complement, the whitened observed data is projected on them:

$$\tilde{\mathbf{X}}_w = (\mathbf{V}_{1:J}^\perp)^H \cdot \mathbf{X}_w \quad (14)$$

Solving a classical  $((K-J) \times (K-J))$  ICA problem for whitened observed data, i.e.  $\tilde{\mathbf{X}}_w = \mathbf{W} \cdot \tilde{\mathbf{X}}$ , the mixing matrix is estimated as:

$$\hat{\mathbf{A}} = \tilde{\mathbf{U}} \cdot \mathbf{Q} \mathbf{S} \cdot \begin{bmatrix} \mathbf{V}_{1:J} & \mathbf{V}_{1:J}^\perp \\ 0 & \mathbf{W} \end{bmatrix} \cdot \begin{bmatrix} \mathbf{I}_{J \times J} & 0 \\ 0 & \mathbf{W} \end{bmatrix} \quad (15)$$

Finally, the sources could be estimated using pseudo-inverse:

$$\hat{\mathbf{S}} = (\hat{\mathbf{A}})^\dagger \cdot \mathbf{X} \quad (16)$$

Equations 10 through 16 represent the main scICA algorithm.

### MIEB as an Enhanced scICA

Here, we plan to develop a new multichannel ICA based beamformer exploiting Lead Field Matrix information. This beamformer, unlike LCMV, estimates few sources simultaneously and it is more robust in reconstructing correlated sources.

The existence of such sources and additive white Gaussian noise violates the main assumption of ICA, i.e. statistical independency. Meanwhile, the iterative procedure which

makes columns of the whitened known vectors, i.e.  $\mathbf{v}_l$ , pairwise orthogonal introduces some errors. These cases weaken the performance of the algorithm, thus we propose not to orthogonalize the column vectors of  $\mathbf{v}_l$  corresponding to correlated sources in order to avoid the error introduced in that step and compensate somehow the assumptions of the problem. At the beginning of the algorithm, the known mixing vectors are arranged in two groups according to their correspondence to correlated or uncorrelated sources. Consequently, Columns of  $\mathbf{v}_l$  in equation (13) the corresponding to the known mixing vectors, and also after normalizing, have already been in an arranged order:

$$\mathbf{v}_l = [\mathbf{v}_{uc} \ \mathbf{v}_c] \quad (17)$$

$\mathbf{v}_{uc}$  is a column wise orthogonalized using based on Procrustes problem [24] using an iterative procedure by minimizing the below function :

$$\|\mathbf{v}_i \cdot \mathbf{D} - \mathbf{Z}\|^2, \quad i = 1, \dots, N_{uc} \quad (18)$$

and  $\mathbf{v}_c$  remains intact:

$$\mathbf{v}_c = \mathbf{v}_i, \quad i = 1, \dots, N_c \quad (19)$$

$N_c$  and  $N_{uc}$  are the number of correlated and uncorrelated sources, respectively and  $N_{uc} + N_c = J$ .

Moreover, it is recommended to use ‘‘JADE’’ rather than ‘‘SOBI’’ in solving classical  $J$ - $K$  ICA problem because the latter is not that effective when sources are mutually correlated.

Our modified algorithm (MIEB) can be summarized as follows which has been modified mainly in steps 1, 8 and 10 compared to scICA [17].

#### MIEB Algorithm

1. Sort mixing vectors into two groups and put them in a matrix; then compute its orthogonal basis,  $\tilde{\mathbf{U}}_{1:J}$ .
2. Project the data on the orthogonal comple-

ment of  $\tilde{\mathbf{U}}_{1:J}$ . Call this data  $\mathbf{X}_2$ .

3. Compute the  $K$ - $J$  dominant left singular vectors of  $\mathbf{X}_2$  and stack in  $\tilde{\mathbf{U}}_{(J+1):K}$ .

4. Project the data on  $\tilde{\mathbf{U}}$  in order to obtain the dimension reduced data,  $\mathbf{X}_s$ .

5. Whiten the data:  $\mathbf{X}_w = \mathbf{P}^\dagger \mathbf{Q}^H \cdot \mathbf{X}_s$ , which  $\mathbf{P}$  and  $\mathbf{Q}$  are obtained from eigenvalue decomposition (EVD) of the covariance matrix of  $\mathbf{X}_s$ .

6. Whiten the known vectors as:  $\mathbf{v}_l = \mathbf{P}^\dagger \mathbf{Q}^H \cdot \tilde{\mathbf{U}}^H$ ,  $l = 1 \dots J$ .

7. Normalize  $\mathbf{v}_l$ ,  $l = 1 \dots J$ .

8. Orthogonalize  $\mathbf{v}_l$  for,  $l = 1 \dots N_{uc}$  iteratively as follows:

a)  $\mathbf{v}_{1:N_{uc}} \cdot \mathbf{D} = \mathbf{A} \mathbf{C} \mathbf{B}^H \rightarrow \mathbf{Z} = \mathbf{A} \mathbf{B}^H$ .

b)  $\mathbf{D} = (\text{diag}(\mathbf{Z}^H \mathbf{v}_{1:N_{uc}}))^{-1}$ .

9. Project  $\mathbf{X}_w$  on the orthogonal complement of  $\mathbf{v}_j$ ; call the new data  $\tilde{\mathbf{X}}_w$ .

10. Solve ICA problem based on ‘‘JADE’’ al-

gorithm  $\tilde{\mathbf{X}}_w = \mathbf{W} \cdot \tilde{\mathbf{X}}$ .

11. Determine the overall mixing matrix as

$$\hat{\mathbf{A}} = \tilde{\mathbf{U}} \cdot \mathbf{Q} \mathbf{S} \cdot \begin{bmatrix} \mathbf{V}_{1:J} & \mathbf{V}_{1:J}^\perp \\ \mathbf{0} & \mathbf{W} \end{bmatrix}$$

12. Estimate the sources of interest:

$$\hat{\mathbf{S}} = (\hat{\mathbf{A}})^\dagger \cdot \mathbf{X}$$

### Results

The concept of EEG forward and inverse problems are shown schematically in Figure 1. In order to check the performance of the enhanced MIEB algorithm, we build a simulation environment and acquired synthetic EEG data. First, we build a 3-layer boundary element method (BEM) model representing scalp, skull and brain as the forward solution implemented in the Field-Trip toolbox [25]. The conductivity value of scalp, skull and brain were 0.3300, 0.0042 and 0.3300 S/m, respectively. Totally 200 nodes out of about 2500 node of the canonical cortical mesh were selected randomly as source locations, 15 of which were supposed to be dominant brain dipole sources with considerably high amplitude and the rest was considered to be as non-dominant neural noise with negligible power. The

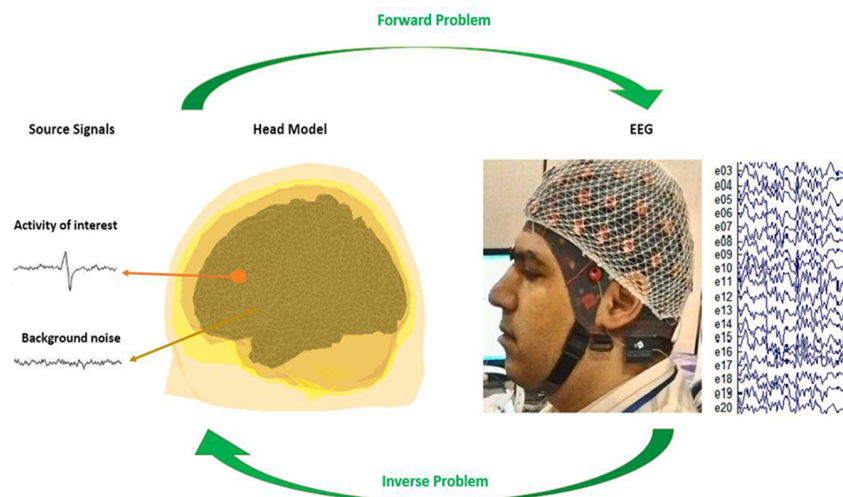


**Figure 1:** Schematic representation of electroencephalogram (EEG) forward and inverse problems.

orientation of the whole dipoles was supposed to be perpendicular to the cortical layer. Also, it was supposed that prior location information for 7 sources, out of the 15 dominant sources, is known through the lead field matrix. We call these 7 sources as desired known ones. Three of the known sources were simulating the delta, alpha, and beta rhythms which were produced by filtering the white noise in the relevant frequency band.

In order to build temporally overlapped correlated version of a brain rhythm, we applied a short FIR filter, with specific coefficients, on the original rhythm source signal. Moreover, in order to generate random correlated sources, we used copulas. Using a copula function makes us be able to construct a bivariate distribution by specifying marginal distributions and an arbitrary level of correlation structure between them [26]. These sources may not have a linear correlation but are more representative of dependent sources. Therefore, the last 2 known sources were randomly distributed no matter how correlated they are.

Solving the forward problem in a standard 32-channel EEG recording arrangement, scalp EEG leads to which a white Gaussian noise added to represent the sensor level noise. Figure 2 sketches the 3-layer head forward model, geometry of sources and sensors in simulated space.

The simulated experiments were done in noise-free and noisy conditions. For noisy cases, two types of noise were considered:

1. Additive white Gaussian noise with Signal to Noise Ratio (SNR) equal to 30 dB. SNR is defined as the ratio of signal power to noise power in dB:

$$SNR = 10 \log_{10} \left( \frac{X^2/N^2}{N^2} \right) \quad (20)$$

2. Embedded neural noise, which simulates the weak effect of adjacent neural activities with variance equal to 0.01.

To evaluate the quality of the reconstructed time course of the source, we used normalized mean squared error defined as follows:

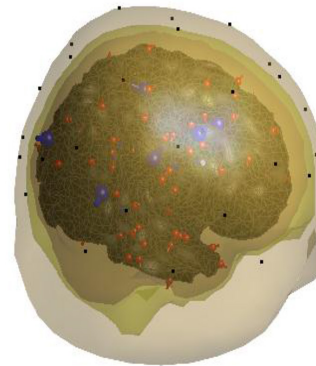


**Figure 2:** A 3-layer boundary element model of head and dipoles' position and orientation overlaid on it. Red: Noise neural dipoles. Blue: Dominant neural dipoles. Black: the position of the electrodes.

$$NMSE = \left\| \frac{\mathbf{s}(\mathbf{r})}{\|\mathbf{s}(\mathbf{r})\|_{\ell_2}} - \frac{\hat{\mathbf{s}}(\mathbf{r})}{\|\hat{\mathbf{s}}(\mathbf{r})\|_{\ell_2}} \right\|_{\ell_2} \quad (21)$$

where  $\mathbf{s}(\mathbf{r})$  and  $\hat{\mathbf{s}}(\mathbf{r})$  are the original and reconstructed time course of the source, respectively.

Figures 3 and 4 show mean and variance of the error after running the simulation for 100 times, in noise-free and noisy conditions, respectively.

As Figure 3 shows, LCMV lacks acceptable performance in the case of correlated sources. The variance of error is trivial for all the method. In reconstruction of correlated sources, scICA outperforms LCMV and DCBF which are originally developed for recovery of correlated sources. DCBF acts well when sources have time-overlap correlation, but in the case of random dependent sources it fails. MIEB has the minimum mean recovery error in the case of both uncorrelated and correlated sources. Clearly, its performance is not dependent on the source correlation.

To make the conditions more realistic, we add two kinds of noise to the data as discussed above. Apparently, the mean error of the whole methods has increased and MIEB seems to have more NMSE variance. In the case of temporally overlapped correlated sources, MIEB

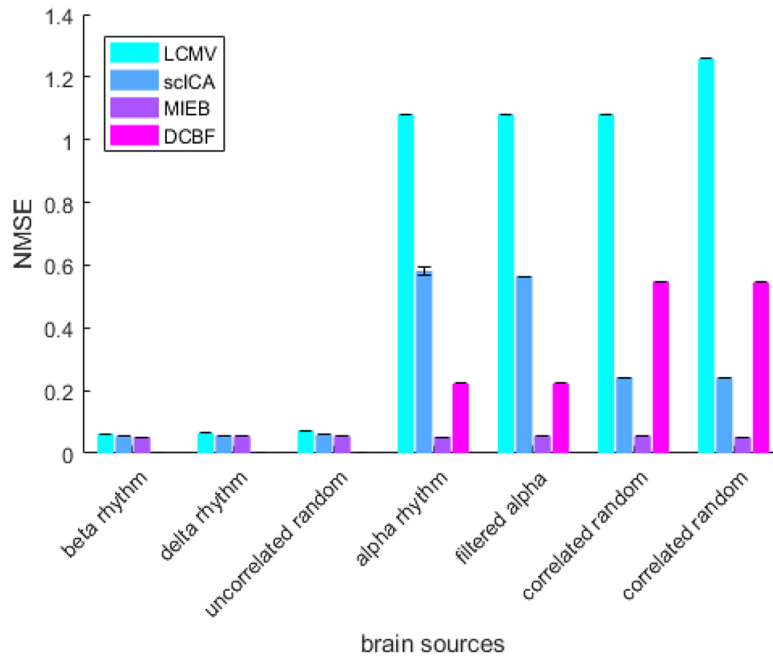


**Figure 3:** Mean and variance of normalized mean squared error (NMSE) of recovered source signals over 100 noise-free case experiments.

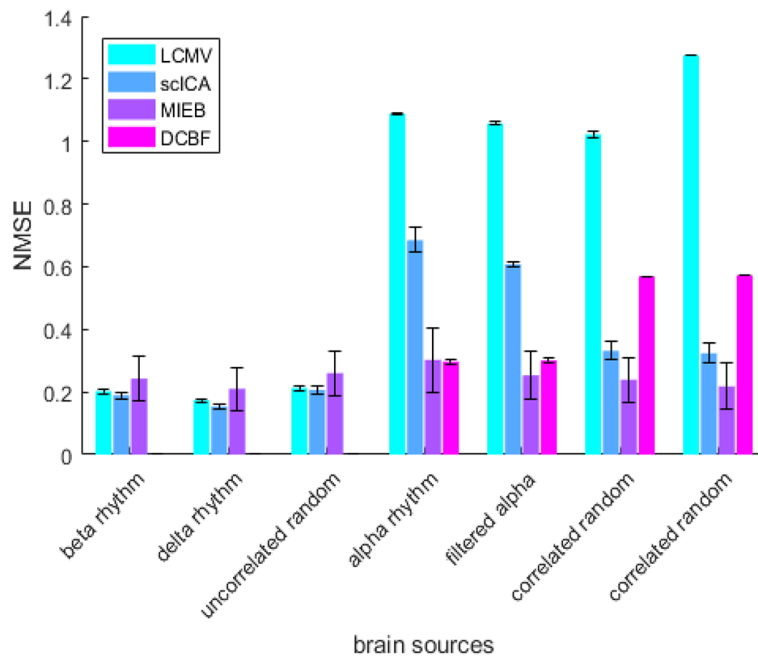


**Figure 4:** Mean and variance of normalized mean squared error (NMSE) of recovered source signals over 100 noisy case experiments.

acts better than scICA but almost has the same performance as DCBF, but MIEB has much less error than DCBF in recovering random correlated sources even considering its relatively high variance.

We came to this conclusion that if high SNR EEG signals are available and a prior spatial information about the location of the neural sources in the brain is known, then the proposed MIEB algorithm can be used to reconstruct the activity of the sources. It has better performance in comparison with the conventional LCMV and even DCBF which is dedicatedly developed to solve the correlation problem.

## Discussion

In this paper, we tried to look at the problem of EEG source imaging from a BSS-based point of view which is possible by replacing the mixing matrix with the lead field matrix. This leads to a Multichannel ICA based EEG Beamformer (MIEB) that reconstructs the arbitrary number of sources simultaneously and its performance was enhanced by modifying the proposed algorithm in [17] as mentioned section 2.3. The mentioned algorithm has the application in EEG neural source recovery especially in the case of correlated sources. As results demonstrate the proposed algorithm has much better performance in comparison with conventional LCMV beamformer as well as to its original version introduced in [17] especially in reconstructing correlated EEG sources.

It is suggested for the future to work much more on different statistical conditions such as correlation, independency as well as an optimum method for estimating the number of sources and including these parameters as prior information in the main algorithm. Also, we propose testing the algorithms on real EEG data and evaluating the source real statistical distribution by realistic head models and experimental data.

## Conclusion

The proposed Multichannel ICA based EEG Beamformer (MIEB) reconstructs the arbitrary number of EEG sources simultaneously. In a simulation environment, we generated synthetic EEG data and demonstrated that it has less reconstruction error than scICA, LCMV, and DCBF in terms of NMSE especially for correlated sources.

## Acknowledgment

This study is part of a PhD thesis supported by Tehran University of Medical sciences (grant No: 95-01-30-31612).

This study is also supported by Cognitive Sciences and Technologies Council under tracking codes 4517 and 4907.

## Conflict of Interest

None

## References

1. Acar ZA, Makeig S. Neuroelectromagnetic forward head modeling toolbox. *J Neurosci Methods*. 2010;**190**:258-70. doi: 10.1016/j.jneumeth.2010.04.031. PubMed PMID: 20457183. PubMed PMCID: PMC4126205.
2. Hallez H, Vanrumste B, Grech R, Muscat J, De Clercq W, Vergult A, et al. Review on solving the forward problem in EEG source analysis. *J Neuroeng Rehabil*. 2007;**4**:46. doi: 10.1186/1743-0003-4-46. PubMed PMID: 18053144. PubMed PMCID: PMC2234413.
3. Grech R, Cassar T, Muscat J, Camilleri KP, Fabri SG, Zervakis M, et al. Review on solving the inverse problem in EEG source analysis. *J Neuroeng Rehabil*. 2008;**5**:25. doi: 10.1186/1743-0003-5-25. PubMed PMID: 18990257. PubMed PMCID: PMC2605581.
4. Pascual-Marqui RD. Review of methods for solving the EEG inverse problem. *Int J Bioelectromagn*. 1999;**1**:75-86.
5. Mosher JC, Lewis PS, Leahy RM. Multiple dipole modeling and localization from spatio-temporal MEG data. *IEEE Trans Biomed Eng*. 1992;**39**:541-57. doi: 10.1109/10.141192. PubMed PMID: 1601435.
6. Sekihara K, Nagarajan SS. Adaptive spatial filters for electromagnetic brain imaging. Berlin:

- Springer Science & Business Media; 2008.
7. Jonmohamadi Y, Poudel G, Innes C, Weiss D, Krueger R, Jones R. Comparison of beamformers for EEG source signal reconstruction. *Biomed Signal Process Control*. 2014;**14**:175-88.
  8. Murzin V, Fuchs A, Scott Kelso JA. Detection of correlated sources in EEG using combination of beamforming and surface Laplacian methods. *J Neurosci Methods*. 2013;**218**:96-102. doi: 10.1016/j.jneumeth.2013.05.001. PubMed PMID: 23769770. PubMed PMCID: PMC3742082.
  9. Diwakar M, Huang MX, Srinivasan R, Harrington DL, Robb A, Angeles A, et al. Dual-Core Beamformer for obtaining highly correlated neuronal networks in MEG. *Neuroimage*. 2011;**54**:253-63. doi: 10.1016/j.neuroimage.2010.07.023. PubMed PMID: 20643211.
  10. Georgieva P, Bouaynaya N, Silva F, Mihaylova L, Jain LC. A Beamformer-Particle Filter Framework for Localization of Correlated EEG Sources. *IEEE J Biomed Health Inform*. 2016;**20**:880-92. doi: 10.1109/JBHI.2015.2413752. PubMed PMID: 25794405.
  11. Brookes MJ, Stevenson CM, Barnes GR, Hillbrand A, Simpson MI, Francis ST, et al. Beamformer reconstruction of correlated sources using a modified source model. *Neuroimage*. 2007;**34**:1454-65. doi: 10.1016/j.neuroimage.2006.11.012. PubMed PMID: 17196835.
  12. Van Veen BD, Van Drongelen W, Yuchtman M, Suzuki A. Localization of brain electrical activity via linearly constrained minimum variance spatial filtering. *IEEE Trans Biomed Eng*. 1997;**44**:867-80. doi: 10.1109/10.623056. PubMed PMID: 9282479.
  13. Sekihara K, Nagarajan SS. Electromagnetic brain imaging: a bayesian perspective. New York: Springer; 2015.
  14. Sekihara K, Nagarajan SS, Poeppel D, Marantz A. Performance of an MEG adaptive-beamformer technique in the presence of correlated neural activities: effects on signal intensity and time-course estimates. *IEEE Trans Biomed Eng*. 2002;**49**:1534-46. PubMed PMID: 12549735.
  15. James CJ, Gibson OJ. Temporally constrained ICA: an application to artifact rejection in electromagnetic brain signal analysis. *IEEE Trans Biomed Eng*. 2003;**50**:1108-16. doi: 10.1109/TBME.2003.816076. PubMed PMID: 12943278.
  16. Hesse CW, James CJ. On semi-blind source separation using spatial constraints with applications in EEG analysis. *IEEE Trans Biomed Eng*. 2006;**53**:2525-34. doi: 10.1109/TBME.2006.883796. PubMed PMID: 17153210.
  17. De Vos M, De Lathauwer L, Van Huffel S. Spatially constrained ICA algorithm with an application in EEG processing. *Signal Processing*. 2011;**91**:1963-72.
  18. Cichocki A, Amari S-I. Adaptive blind signal and image processing: learning algorithms and applications. New Jersey: John Wiley & Sons; 2002.
  19. Oja H, Nordhausen K. Independent component analysis. *Encyclopedia of Environmetrics*. 2013. doi: 10.1002/9780470057339.vnn086.
  20. Cardoso J-F, Souloumiac A. Blind beamforming for non-Gaussian signals. *IEE Proceedings F (Radar and Signal Processing)*. 1993;**140**:362-70.
  21. Belouchrani A, Abed-Meraim K, Cardoso J-F, Moulines E. A blind source separation technique using second-order statistics. *IEEE Trans Signal Process*. 1997;**45**:434-44.
  22. Hyvarinen A. Fast and robust fixed-point algorithms for independent component analysis. *IEEE Trans Neural Netw*. 1999;**10**:626-34. doi: 10.1109/72.761722. PubMed PMID: 18252563.
  23. Roberts SJ. Independent component analysis: source assessment and separation, a Bayesian approach. *IEE Proceedings-Vision, Image and Signal Processing*. 1998;**145**:149-54.
  24. Golub GH, Van Loan CF. Matrix computations. 4th ed. Baltimore: Johns Hopkins University Press; 2013.
  25. Oostenveld R, Fries P, Maris E, Schoffelen JM. FieldTrip: Open source software for advanced analysis of MEG, EEG, and invasive electrophysiological data. *Comput Intell Neurosci*. 2011;**2011**:156869. doi: 10.1155/2011/156869. PubMed PMID: 21253357. PubMed PMCID: PMC3021840.
  26. Assecondi S, Ostwald D, Bagshaw AP. Reliability of information-based integration of EEG and fMRI data: a simulation study. *Neural Comput*. 2015;**27**:281-305. doi: 10.1162/NECO\_a\_00695. PubMed PMID: 25514112.